

## Crystal structures and magnetic properties of zircon-type compounds

 $\text{Lu}_{1-x}\text{Y}_x\text{CrO}_4$ Keitaro Tezuka,<sup>†</sup> Yoshihiro Doi and Yukio Hinatsu

Division of Chemistry, Graduate School of Science, Hokkaido University, Sapporo 060-0810, Japan

Received 18th September 2001, Accepted 4th January 2002

First published as an Advance Article on the web 25th February 2002

We prepared solid solutions of antiferromagnetic  $\text{LuCrO}_4$  and ferromagnetic  $\text{YCrO}_4$ , *i.e.*,  $\text{Lu}_{1-x}\text{Y}_x\text{CrO}_4$  ( $x = 0-1.0$  at 0.125 intervals). Their precise crystal structures were determined from the X-ray diffraction measurements. All the solid solutions have a zircon-type structure with space group  $I4_1/amd$  (No. 141). Their magnetic susceptibility measurements have been performed in the temperature range between 1.8 K and 300 K. The solid solutions for  $x = 0-0.375$  show an antiferromagnetic transition and those for  $x = 0.5-1.0$  show a ferromagnetic transition at low temperatures. It was found that the magnetic transition temperatures for the solid solutions were lower than those for pure  $\text{LuCrO}_4$  (9.1 K) and  $\text{YCrO}_4$  (9.2 K), and the Curie temperature for  $\text{Lu}_{0.5}\text{Y}_{0.5}\text{CrO}_4$  is the lowest (5.2 K). The magnetization curves indicate the occurrence of metamagnetism for  $\text{Lu}_{0.75}\text{Y}_{0.25}\text{CrO}_4$  and  $\text{Lu}_{0.625}\text{Y}_{0.375}\text{CrO}_4$ . Specific heat measurements have been performed for  $\text{Lu}_{1-x}\text{Y}_x\text{CrO}_4$  ( $x = 0, 0.375, 0.5, 1$ ) in the temperature range between 1.8 K and 300 K.  $\lambda$ -Type anomalies have been found at their magnetic transition temperatures. Magnetic entropy change due to magnetic exchange interactions has been evaluated from the specific data.

## Introduction

It is known that  $\text{RCrO}_4$  ( $R = \text{Nd-Lu, Y}$ ) have a zircon-type structure with space group  $I4_1/amd$  (No. 141).<sup>1,2</sup> All of them have a long range magnetic ordering at low temperatures.<sup>3-6</sup> The compounds for  $R = \text{Nd-Eu, Lu}$  are antiferromagnetic and those for  $R = \text{Gd-Yb}$  are ferromagnetic below 9–24 K.

In the case of  $\text{LuCrO}_4$  and  $\text{YCrO}_4$ , their magnetic properties are ascribable to the behavior of  $\text{Cr}^{5+}$  ions in solids, because  $\text{Lu}^{3+}$  and  $\text{Y}^{3+}$  ions are diamagnetic. The magnetic properties were investigated by magnetic susceptibility measurements for  $\text{LuCrO}_4$ <sup>6</sup> and by specific heat and magnetization measurements below 30 K for  $\text{YCrO}_4$ .<sup>4</sup> As a result, it was found that the magnetic properties were very different between them, *i.e.*,  $\text{LuCrO}_4$  showed an antiferromagnetic transition below 9.9 K,<sup>6</sup> and  $\text{YCrO}_4$  showed a ferromagnetic transition below 9.2 K.<sup>4</sup>

Since the crystal structures of these two compounds are the same, the formation of solid solutions  $\text{Lu}_{1-x}\text{Y}_x\text{CrO}_4$  is expected over a wide range of  $x$ . Through magnetic studies, we can investigate the magnetic properties of these solid solutions and may obtain information as to what is responsible for the difference in the magnetic properties of  $\text{LuCrO}_4$  and  $\text{YCrO}_4$ .

In this study, we prepared solid solutions  $\text{Lu}_{1-x}\text{Y}_x\text{CrO}_4$ , and have performed their detailed crystallographic and magnetic studies, using X-ray diffraction, magnetic susceptibility, and specific heat measurements. We will discuss their results here.

## Experimental

Solid solutions  $\text{Lu}_{1-x}\text{Y}_x\text{CrO}_4$  ( $x = 0-1.0$  at intervals of 0.125) were prepared. Starting materials were  $\text{R}_2\text{O}_3$  ( $R = \text{Lu and Y}$ ) and  $\text{Cr}(\text{NO}_3)_3 \cdot 9\text{H}_2\text{O}$ . These materials were weighed in the correct ratios and dissolved in conc. nitric acid. The nitric solutions were evaporated, and the obtained nitrates were

heated in a flow of oxygen gas at 160 °C for 1 h, 200 °C for 2 h and 600 °C for 4 h. After cooling, they were ground and heated in a flow of oxygen gas at 600 °C for 4 h. The low preparation temperature 600 °C was employed in this study, because higher temperature causes the reduction of  $\text{Cr}^{5+}$  ions.

Powder X-ray diffraction patterns were measured with  $\text{Cu-K}\alpha$  radiation on a Rigaku RINT2000 diffractometer. The structures were refined with the Rietveld analysis method, using program RIETAN.<sup>7</sup>

Magnetic susceptibilities were measured with a SQUID magnetometer (Quantum Design, MPMS model) after zero field cooling (ZFC) and field cooling (FC) processes in the temperature range 1.8–300 K. The former was measured upon heating the sample to 300 K under the applied magnetic field of 0.1 T after zero-field cooling to 1.8 K. The latter was measured upon cooling the sample from 300 K to 1.8 K at 0.1 T. The field dependence of the magnetization was measured at 1.8 K by changing the magnetic field strength in the range between –5 T and 5 T.

Specific heat measurements were performed using a relaxation technique by the commercial specific heat measuring system (Quantum Design, PPMS) in the temperature range 1.8–300 K. The sample in the form of a pellet was mounted on a thin alumina plate with apiezon for better thermal contact.

## Results and discussion

## Crystal structure

The  $\text{Lu}_{1-x}\text{Y}_x\text{CrO}_4$  systems form a solid solution phase with a tetragonal zircon-type structure over a range of  $0 \leq x \leq 1$ . Their X-ray diffraction profiles were indexed with a tetragonal unit cell, space group  $I4_1/amd$  (No. 141) for  $x = 0-1$ . Fig. 1 shows the diffraction pattern for  $\text{YCrO}_4$ , as an example. The structural refinements were performed by means of the Rietveld method. The results (lattice parameters and atomic positions) are shown in Table 1. With increasing Y concentration in the  $\text{Lu}_{1-x}\text{Y}_x\text{CrO}_4$  solid solutions, both the lattice parameters  $a$  and  $c$  become larger, which is shown in Fig. 2. This trend is easily

<sup>†</sup>Present address: Department of Applied Chemistry, Faculty of Engineering, Utsunomiya University, Yoto, Utsunomiya 321-8585, Japan.

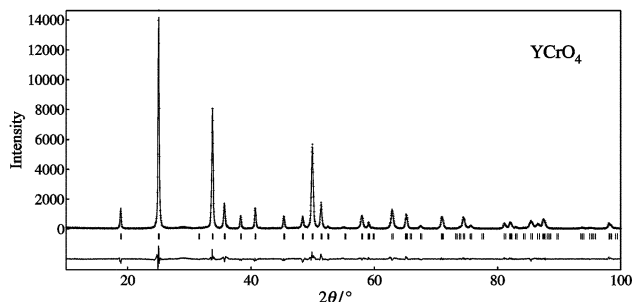


**Fig. 1** Powder X-ray diffraction pattern fitting for  $\text{YCrO}_4$ . The calculated and observed patterns are shown on the top solid line and the markers above the peaks, respectively. The vertical marks in the middle show positions calculated for Bragg reflections. The lower trace is a plot of the difference between calculated and observed intensities.

**Table 1** Lattice parameters and atomic positions for  $\text{Lu}_{1-x}\text{Y}_x\text{CrO}_4$  ( $x = 0-1$ )<sup>a</sup>

$x$	0	0.25	0.50	0.75	1.0
$a/\text{Å}$	7.0186(5)	7.0448(5)	7.0682(5)	7.0948(5)	7.1162(5)
$c/\text{Å}$	6.1900(4)	6.2085(5)	6.2234(5)	6.2414(5)	6.2543(4)
$y$ (O)	0.180(1)	0.180(1)	0.179(1)	0.180(1)	0.179(1)
$z$ (O)	0.331(1)	0.332(1)	0.331(1)	0.331(1)	0.330(1)
$B/\text{Å}^2$ (Lu/Y)	0.52	0.62	0.47	0.60	0.52
$B/\text{Å}^2$ (Cr)	0.44	0.49	0.40	0.45	0.43
$B/\text{Å}^2$ (O)	1.09	1.00	1.08	0.98	0.96
$R_{\text{wp}}(\%)$	9.07	9.06	9.29	9.52	9.90
$R_{\text{I}}(\%)$	2.91	3.89	3.16	2.47	2.22
$R_{\text{F}}(\%)$	1.44	2.24	1.90	1.40	0.94

<sup>a</sup>Atomic positions are Lu/Y on  $4a$  (0,0,0), Cr on  $4b$  (0,0,1/2), and O on  $16h$  (0, $y$ , $z$ ) of space group  $I4_1/amd$  (No. 141). Definitions of reliability factors  $R_{\text{wp}}$ ,  $R_{\text{I}}$  and  $R_{\text{F}}$  are given as follows:  $R_{\text{wp}} = \sum_i w_i (y_i - y_{\text{ci}})^2 / \sum_i w_i y_i^2$ ,  $R_{\text{I}} = \sum_k |I_k(\text{obs}) - I_k(\text{cal})| / \sum_k I_k(\text{obs})$  and  $R_{\text{F}} = \sum_k |(I_k(\text{obs}))^{1/2} - (I_k(\text{calc}))^{1/2}| / \sum_k (I_k(\text{obs}))^{1/2}$ .

understandable by considering the ionic radius of  $\text{Lu}^{3+}$  and  $\text{Y}^{3+}$ .<sup>8</sup> Fig. 3 shows its crystal structure. In these  $\text{Lu}_{1-x}\text{Y}_x\text{CrO}_4$  compounds, the rare earth ions are eight-coordinated by oxygen ions, and the chromium ions are four-coordinated by oxygen ions. Some selected bond lengths and angles are listed in Table 2. Both the Lu/Y–O and Cr–O distances increase with substitution of  $\text{Y}^{3+}$  for  $\text{Lu}^{3+}$ . This behavior is due to the fact that the atomic positions of Lu/Y, Cr, and O are unchangeable, although the lattice parameters  $a$  and  $c$  of  $\text{Lu}_{1-x}\text{Y}_x\text{CrO}_4$  increase with  $x$  value.

Specific heat measurements on  $\text{LuCrO}_4$  and  $\text{YCrO}_4$ , and

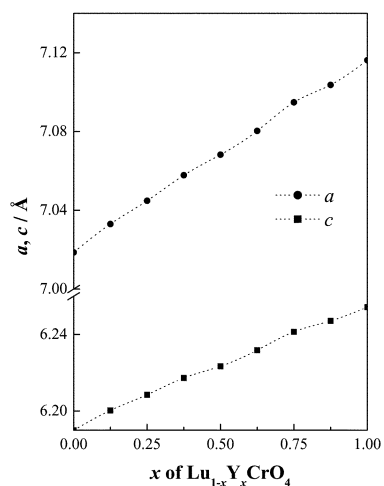


**Fig. 2** Lattice parameters for  $\text{Lu}_{1-x}\text{Y}_x\text{CrO}_4$ . Broken lines are guides to the eye.

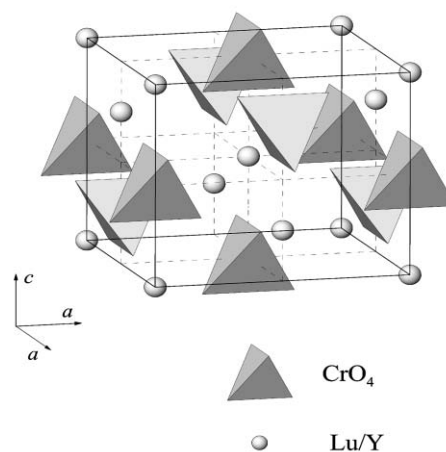


**Fig. 3** The crystal structure of  $\text{Lu}_{1-x}\text{Y}_x\text{CrO}_4$ .

**Table 2** Bond lengths (Å) and angles (°) for  $\text{Lu}_{1-x}\text{Y}_x\text{CrO}_4$  ( $x = 0-1$ )

$x$	0	0.25	0.5	0.75	1.0
Lu/Y–O × 4	2.302(3)	2.311(3)	2.318(3)	2.327(3)	2.336(2)
Lu/Y–O × 4	2.408(4)	2.417(3)	2.419(3)	2.422(3)	2.427(2)
Cr–O × 4	1.639(3)	1.644(3)	1.651(3)	1.657(2)	1.661(2)
Lu/Y–O–Lu/Y × 8	109.0(1)	109.0(1)	109.2(1)	109.1(1)	109.3(1)
Lu/Y–O–Cr × 4	98.0(2)	97.9(2)	98.0(2)	97.9(1)	98.1(1)
Lu/Y–O–Cr × 4	153.0(1)	153.1(2)	152.9(2)	152.9(2)	152.6(1)

their solid solutions show that no structural phase transition is observed in the temperature range 1.8–300 K. In the  $\text{DyCrO}_4$  compound, a tetragonal to orthorhombic phase transition has been observed with decreasing temperature.<sup>3</sup>

### Magnetic properties

**$\text{LuCrO}_4$ .** Fig. 4 shows the inverse magnetic susceptibility of  $\text{LuCrO}_4$  as a function of temperature and the inset shows the

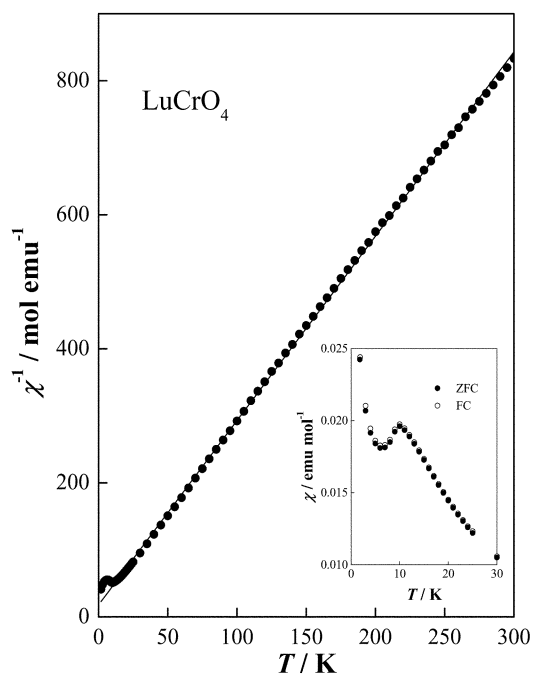


**Fig. 4** Temperature dependence of inverse magnetic susceptibilities for  $\text{LuCrO}_4$ . A solid line represents the Curie–Weiss fitting. The inset shows the magnetic susceptibilities as a function of temperature in a lower temperature region.

temperature dependence of the magnetic susceptibility in the low temperature region. An antiferromagnetic transition is observed at 9.1 K, which is close to the value 9.9 K reported previously.<sup>6</sup> Below the Néel temperature, no difference between the ZFC and FC magnetic susceptibilities is observed, indicating that a ferromagnetic component does not exist in the antiferromagnetic properties of LuCrO<sub>4</sub>. The susceptibility obeys the Curie–Weiss law above 30 K. The effective magnetic moment is determined to be 1.71  $\mu_B$ , which agrees well with the moment calculated by considering the contribution of Cr<sup>5+</sup> (3d<sup>1</sup>) with  $S = 1/2$  (1.73  $\mu_B$ ). This result confirms that the chromium ion in LuCrO<sub>4</sub> is in the pentavalent state. The Weiss constant is determined to be –6.5 K, indicating the existence of antiferromagnetic interactions.

In order to investigate the antiferromagnetic transition at 9.1 K in detail, specific heat measurements have been performed. Fig. 5 shows the variation of specific heat as a function of temperature. The  $\lambda$ -type anomaly (which means the existence of a magnetic transition) has been found at 9.2 K, which corresponds to the antiferromagnetic transition found in the susceptibility vs. temperature curve.

To calculate the magnetic contribution to the specific heat, we subtract the electronic and lattice contributions from the total specific heat. It is known that the electronic and lattice contribution to the specific heat is proportional to the temperature and three powers of temperature, respectively. We evaluate the components of the electronic and lattice contribution by fitting the observed specific heat to the function  $f(T) = a \times T + b \times T^2 + c \times T^3$  in the temperature range  $30 \text{ K} < T < 50 \text{ K}$  where little influence of the magnetic transition is expected. The inset in Fig. 5 shows the magnetic specific heat  $C_m$  of LuCrO<sub>4</sub> divided by temperature as a function of temperature.

The entropy change due to the magnetic transition  $\Delta S_m$  is obtained to be 4.34 J mol<sup>-1</sup> K<sup>-1</sup>, which is near to  $R \ln(2S + 1) = R \ln 2 = 5.76 \text{ J mol}^{-1} \text{ K}^{-1}$ , indicating that only two energy levels are involved in the process of magnetic ordering of Cr, *i.e.*, the ground state of Cr is a doublet. No anomaly corresponding to a structural phase transition such as is found

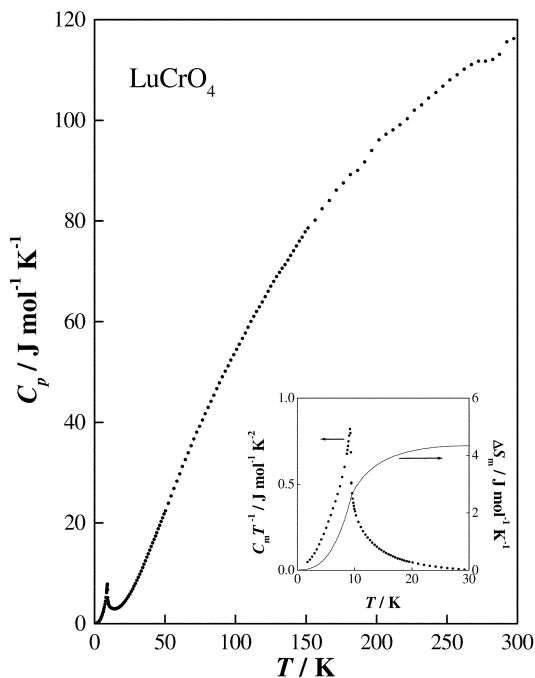


**Fig. 5** Total specific heat  $C_p$  of LuCrO<sub>4</sub> as a function of temperature. The inset shows the magnetic specific heat  $C_m$  of LuCrO<sub>4</sub> divided by temperature as a function of temperature. The solid line represents the magnetic contribution of the entropy  $\Delta S_m$  (right ordinate) as a function of temperature.

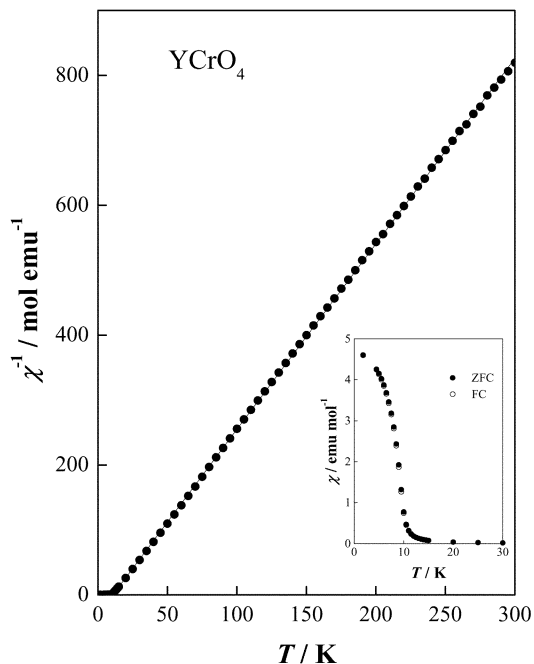


**Fig. 6** Temperature dependence of inverse magnetic susceptibilities for YCrO<sub>4</sub>. The inset shows the magnetic susceptibility vs. temperature curve in a lower temperature region.

in DyCrO<sub>4</sub><sup>3</sup> was observed from the specific heat measurements in the temperature range 1.8 K–300 K.

**YCrO<sub>4</sub>.** Fig. 6 shows the temperature dependence of the inverse magnetic susceptibility of YCrO<sub>4</sub> and the inset shows the temperature dependence of the magnetic susceptibility. A ferromagnetic transition is observed at 9.2 K, which is consistent with the previous result.<sup>4</sup> The susceptibility obeys the Curie–Weiss law above 30 K. The effective magnetic moment is determined to be 1.67  $\mu_B$ , which agrees well with the calculated moment of Cr<sup>5+</sup> with  $S = 1/2$  in YCrO<sub>4</sub> (1.73  $\mu_B$ ). This result also indicates that the chromium ion in YCrO<sub>4</sub> is in the pentavalent state. The Weiss constant is determined to be 10.7 K, indicating the existence of ferromagnetic interactions.

In order to investigate the ferromagnetic component for YCrO<sub>4</sub>, the magnetization measurements were performed at 1.8 K. Fig. 7 shows the magnetization per mole of YCrO<sub>4</sub> as a function of  $H$ . The magnetization increases very rapidly with applied magnetic field, and the saturation value is determined to be 0.87  $\mu_B$ , which is near to the moment of Cr<sup>5+</sup> with  $S = 1/2$  (1.00  $\mu_B$ ).

Fig. 8 shows the temperature dependence of specific heat for YCrO<sub>4</sub>. A  $\lambda$ -type anomaly has been found at 9.1 K, which is

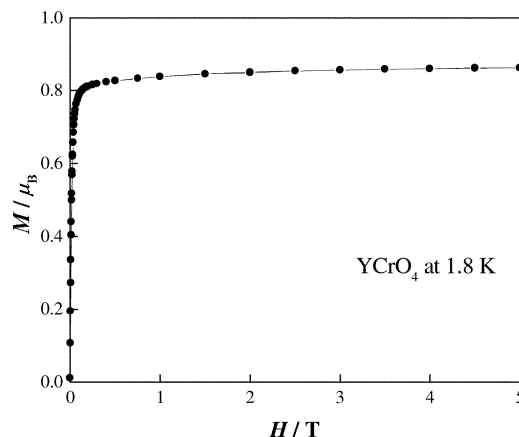


**Fig. 7** Magnetization curve for YCrO<sub>4</sub> at 1.8 K.

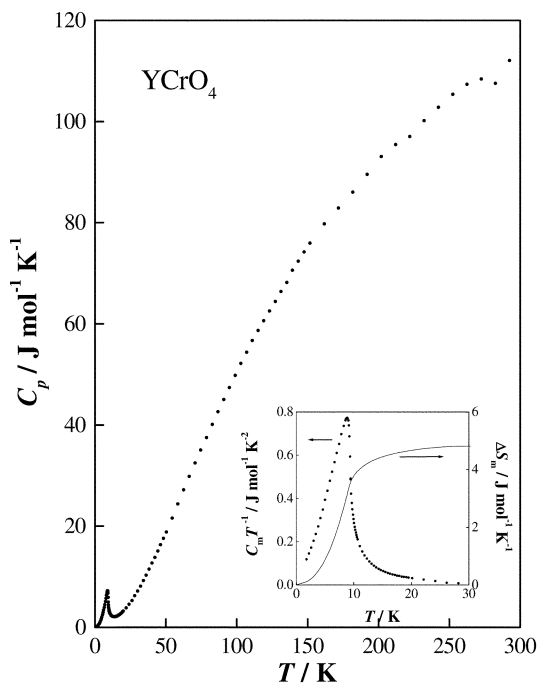


**Fig. 8** Temperature dependence of total specific heat  $C_p$  for  $\text{YCrO}_4$ . The inset shows the magnetic specific heat  $C_m$  of  $\text{YCrO}_4$  divided by temperature as a function of temperature. The solid line represents the magnetic contribution of the entropy  $\Delta S_m$  (right ordinate) as a function of temperature.

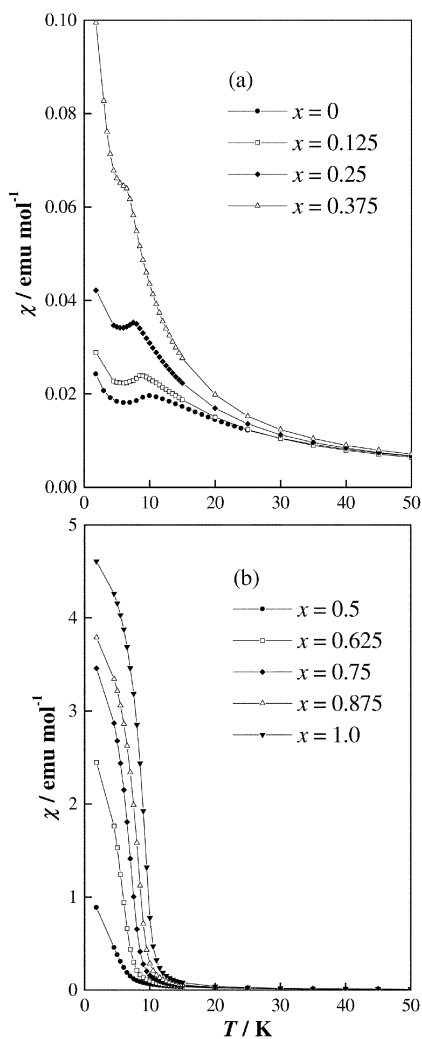


**Fig. 9** Temperature dependence of magnetic susceptibility for  $\text{Lu}_{1-x}\text{Y}_x\text{CrO}_4$ : (a)  $x = 0-0.375$ , (b)  $x = 0.5-1.0$ .

**Table 3** Magnetic properties for  $\text{Lu}_{1-x}\text{Y}_x\text{CrO}_4$  ( $x = 0-1$ )

$x$	Type	$T_N, T_C/\text{K}$	$\mu_{\text{eff}}/\mu_B$	Weiss constant/K
0	Antiferromagnetic	9.1	1.71	-6.5
0.125	Antiferromagnetic	8.2	1.64	-2.4
0.25	Antiferromagnetic	6.8	1.64	-0.2
0.375	Antiferromagnetic	6.0	1.63	3.1
0.5	Ferromagnetic	5.2	1.64	4.9
0.625	Ferromagnetic	5.9	1.64	6.5
0.75	Ferromagnetic	7.1	1.60	7.2
0.875	Ferromagnetic	8.2	1.60	8.9
1.0	Ferromagnetic	9.2	1.67	10.7

consistent with the magnetic susceptibility measurements. The inset in Fig. 8 shows the magnetic specific heat  $C_m$  of  $\text{YCrO}_4$  divided by temperature as a function of temperature. The entropy change due to the magnetic transition  $\Delta S_m$  is obtained to be  $4.82 \text{ J mol}^{-1} \text{ K}^{-1}$ , which is also near to  $R \ln 2 = 5.76 \text{ J mol}^{-1} \text{ K}^{-1}$ , indicating that only two energy levels are involved in the process of magnetic ordering of  $\text{Cr}^{3+}$  ions.

**Solid solutions  $\text{Lu}_{1-x}\text{Y}_x\text{CrO}_4$ .** Temperature dependence of the magnetic susceptibilities for the solid solutions  $\text{Lu}_{1-x}\text{Y}_x\text{CrO}_4$  is shown in Fig. 9(a) and (b). The magnetic properties obtained from these magnetic susceptibility measurements are listed in Table 3.  $\text{LuCrO}_4$  shows an antiferromagnetic transition at 9.2 K. With increasing Y substitution, the Néel temperature  $T_N$  of  $\text{Lu}_{1-x}\text{Y}_x\text{CrO}_4$  becomes lower and it is 6.0 K for  $\text{Lu}_{0.625}\text{Y}_{0.375}\text{CrO}_4$ . Solid solutions  $\text{Lu}_{1-x}\text{Y}_x\text{CrO}_4$  with  $x \geq 0.5$  show ferromagnetic behavior and their Curie temperatures  $T_C$  become higher from 5.2 K for  $\text{Lu}_{0.5}\text{Y}_{0.5}\text{CrO}_4$  to 9.2 K for  $\text{YCrO}_4$ . Fig. 10 shows the variation of the magnetic transition temperature as a function of  $x$  in  $\text{Lu}_{1-x}\text{Y}_x\text{CrO}_4$ . The magnetic transition temperatures for the solid solutions are lower than those for  $\text{LuCrO}_4$  and  $\text{YCrO}_4$ , and the Curie temperature for  $\text{Lu}_{0.5}\text{Y}_{0.5}\text{CrO}_4$  is the lowest. The superexchange interactions are quite complex, since the  $\text{CrO}_4$  tetrahedra are isolated from each other by the diamagnetic  $\text{Lu}/\text{YO}_8$  bisphenoids; the  $\text{Cr}-\text{O}-\text{Cr}$  pathway of superexchange interaction cannot exist in zircon-type compounds  $\text{Lu}_{1-x}\text{Y}_x\text{CrO}_4$ . The probable pathways for this structure are two  $\text{Cr}-\text{O}-\text{Cr}$  and four  $\text{Cr}-\text{O}-\text{Lu}/\text{Y}-\text{O}-\text{Cr}$ .

Fig. 11 shows the detailed magnetization curves at 1.8 K for  $\text{Lu}_{1-x}\text{Y}_x\text{CrO}_4$  ( $x = 0.25, 0.375, 0.5$ ) in the magnetic field ranges of 0–5 T (Fig. 11(a)) and 0–1.5 T (Fig. 11(b)). Fig. 11(a) clearly indicates that the magnetic behavior of  $\text{Lu}_{0.5}\text{Y}_{0.5}\text{CrO}_4$  is ferromagnetic and that there exists a weak ferromagnetic component in the antiferromagnetic interactions for  $\text{Lu}_{0.625}\text{Y}_{0.375}\text{CrO}_4$ . For  $\text{Lu}_{0.75}\text{Y}_{0.25}\text{CrO}_4$  and  $\text{Lu}_{0.625}\text{Y}_{0.375}\text{CrO}_4$ , the

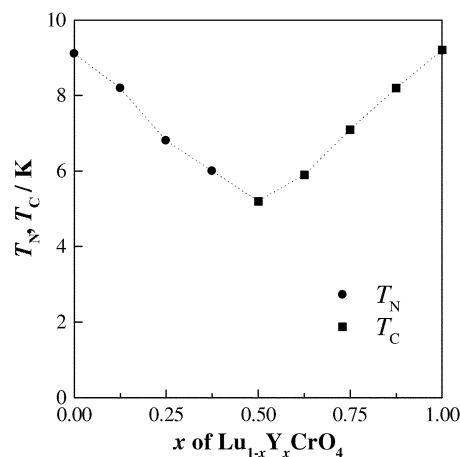


**Fig. 10** The magnetic transition temperature as a function of  $x$  in  $\text{Lu}_{1-x}\text{Y}_x\text{CrO}_4$ .

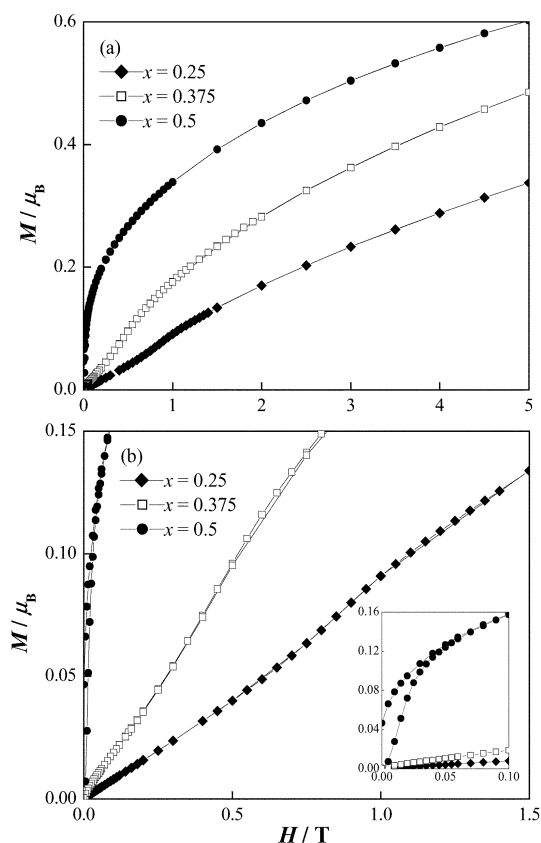


**Fig. 11** Magnetization curves at 1.8 K for  $\text{Lu}_{1-x}\text{Y}_x\text{CrO}_4$  ( $x = 0.25, 0.375, 0.5$ ) in the magnetic field ranges of 0–5 T (a) and 0–1.5 T (b) (inset: 0–0.1 T).

metamagnetic transitions are observed at *ca.* 0.80 T and *ca.* 0.35 T, respectively, from the magnetization curves shown in Fig. 11(b). Their transitions may be due to the spin-flipping.<sup>9</sup>

Fig. 12 shows the temperature dependence of the specific heat for  $\text{Lu}_{0.625}\text{Y}_{0.375}\text{CrO}_4$  and  $\text{Lu}_{0.5}\text{Y}_{0.5}\text{CrO}_4$ . The  $\lambda$ -type anomalies have been observed at 6.0 and 5.2 K, indicating the occurrence of the magnetic transitions in these compounds. These results are in accordance with the results by magnetic susceptibility measurements. The entropy changes due to the magnetic transitions  $\Delta S_m$  for  $\text{Lu}_{0.625}\text{Y}_{0.375}\text{CrO}_4$  and  $\text{Lu}_{0.5}\text{Y}_{0.5}\text{CrO}_4$  are obtained to be  $4.10 \text{ J mol}^{-1} \text{ K}^{-1}$  and  $4.02 \text{ J mol}^{-1} \text{ K}^{-1}$  respectively, indicating that only two energy levels are involved in the process of magnetic ordering of  $\text{Cr}^{5+}$  ions.

## References

- 1 G. Buisson, F. Bertaut and J. Mareschal, *C. R. Hebd. Seances Acad. Sci.*, 1964, **259**, 411.
- 2 G. Buisson, F. Tch ou, F. Sayetat and K. Scheunemann, *Solid State Commun.*, 1976, **18**, 871.
- 3 K. Tezuka and Y. Hinatsu, *J. Solid State Chem.*, 2001, **160**, 362.
- 4 H. Walter, H. G. Kahle, K. Mulder, H. C. Schopper and H. Schwarz, *Int. J. Magn.*, 1973, **5**, 129.
- 5 A. Morales-S anchez, F. Fern andez and R. S aez-Puche, *J. Alloys Compd.*, 1993, **201**, 161.

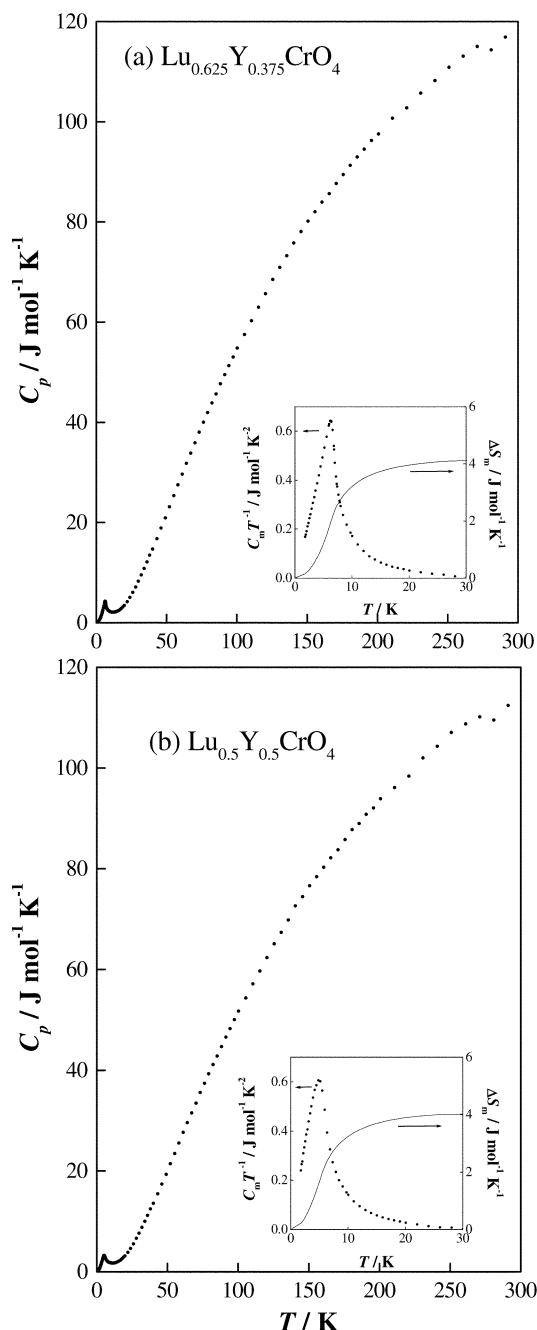


**Fig. 12** Temperature dependence of the specific heat for  $\text{Lu}_{0.625}\text{Y}_{0.375}\text{CrO}_4$  (a) and  $\text{Lu}_{0.5}\text{Y}_{0.5}\text{CrO}_4$  (b). Their insets show the magnetic specific heat  $C_m$  divided by temperature as a function of temperature. The solid lines represent the magnetic contribution of the entropy  $\Delta S_m$  (right ordinate) as a function of temperature.

- 6 E. Jim enez, J. Isasi and R. S aez-Puche, *J. Alloys Compd.*, 2000, **312**, 53.
- 7 F. Izumi, *The Rietveld Method*, ed. R. A. Young, Ch. 13, Oxford University Press, Oxford, 1993.
- 8 R. D. Shannon, *Acta Crystallogr., Sect. A*, 1976, **29**, 751.
- 9 C. J. O'Connor, S. N. Bhatia, R. L. Carlin, A. van der Bilt and A. J. van Duyneveldt, *Physica*, 1978, **95B**, 27.